

The globular cluster system of nearby spirals through multi-band imaging surveys: The case of M 81

J.P. Caso^{1,2}, A.I. Ennis^{3,4}, B.J. De Bórtoli^{1,2}, A.L. Chies-Santos⁵, R.S. de Souza⁶, M. Canossa⁵, P. Floriano⁵, E. Godoy⁵, P. Lopes⁵, N.L. Miranda⁵ & C. Bonato⁵

¹ *Facultad de Ciencias Astronómicas y Geofísicas, UNLP, Argentina*

² *Instituto de Astrofísica de La Plata, CONICET-UNLP, Argentina*

³ *Consejo Nacional de Investigaciones Científicas y Técnicas, Argentina*

⁴ *Waterloo Centre for Astrophysics, University of Waterloo, Canada*

⁵ *Perimeter Institute for Theoretical Physics, Waterloo, Canada*

⁶ *Instituto de Física, UFRGS, Brasil*

⁷ *Shanghai Astronomical Observatory, Chinese Academy of Sciences, China*

Contact / jpcaso@fcaglp.unlp.edu.ar

Resumen / El análisis de los sistemas de cúmulos globulares (SCG) asociados a galaxias espirales cercanas es útil para revelar su historia evolutiva, pero resulta desafiante debido a su gran extensión angular. En la presente contribución nos valemos del gran campo de visión del relevamiento Javalambre Photometric Local Universe Survey (J-PLUS) para encarar el estudio del SCG de la galaxia espiral M 81. Estimamos su extensión y población total, y analizamos su distribución de color.

Abstract / Although the analysis of globular cluster systems (GCSs) in nearby spirals provides relevant information about their evolutionary history, it is challenging because of their angular extension. In this work we take advantage of the large field-of-view of the Javalambre Photometric Local Universe Survey (J-PLUS) to perform a wide-field study of the GCS of the spiral M 81. Its extension and population are estimated, and its colour distribution is analysed.

Keywords / galaxies: star clusters: general — galaxies: spiral — galaxies: groups: individual (M81)

1. Introduction

The assembly of globular cluster systems (GCSs) has proven to be tightly related to the evolutionary processes experienced by their host galaxies (e.g. Kruijssen et al., 2019), and the analysis of their current properties provides valuable information about the mass-growth and star-forming histories of galaxies (Fensch et al., 2020; Villaume et al., 2020). Then, an appropriate study of the GCS is desirable to achieve a comprehensive description of its host galaxy. This is particularly interesting in the case of spirals, since there is a vast number of them with stellar masses above $10^{10} M_{\odot}$, and this abundance produces tension with the hierarchical scenario (Haslbauer et al., 2022, and references there in). Besides the Local Group galaxies, GCSs in spirals have been poorly studied in the literature, and the few analysis that exist usually lack spatial coverage to properly describe the outer regions of the GCSs and to calculate their extension and population (e.g. Nantais et al., 2011; Lomelí-Núñez et al., 2022).

M 81 is a nearby spiral ($D \approx 3.6$ Mpc, Tully et al. 2013), that dominates a group of ≈ 30 members. It constitutes a triplet with the starburst spiral M 82 and the irregular NGC 3077, which are thought to be recently accreted (Oehm et al., 2017). The triplet presents signs of interaction, like bridges in HI connecting the galaxies (de Blok et al., 2018) and low surface-brightness sub-

structure in optical bands (Smercina et al., 2020). Regarding the M 81 GCS, several globular clusters (GCs) have been confirmed as members (Nantais et al., 2010), including some GCs from the outer halo (Perelmuter et al., 1995) and two possible intra-group GCs (Ma et al., 2017).

This contribution continues the analysis of the GCS of the triplet started by Chies-Santos et al. (2022), hereafter Paper I, based on observations from the Javalambre Photometric Local Universe Survey (J-PLUS, Cenarro et al. 2019). The large field-of-view of the survey allows for the analysis of the full extension of the GCS in nearby spirals, and its photometry is deep enough to reach the turn-over magnitude of the GCS at the distance of M 81, which is necessary for an accurate description of the GCS.

2. Observations and photometry

The dataset consists of the processed images in (g, r, i, z) for three pointings from the J-PLUS second data release (DR2), covering the region of the triplet, and spanning to the South, down to a declination of 67.3 deg. The images are downloaded from the J-PLUS collaboration website*.

*http://www.j-plus.es/datareleases/data_release_dr2

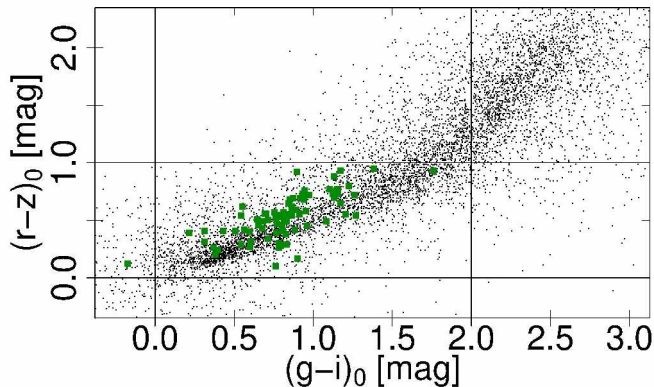


Figure 1: Colour-colour diagram for point-sources, with confirmed GCs from the literature highlighted with green squares. The solid lines represent the colour thresholds.

2.1. Photometry

In order to increase the detection of sources in regions where the surface-brightness is large, the images are pre-processed. A median filter of size 100 px is used to model it on each filter, and then subtracted from the original image. The detection of sources and their aperture photometry are carried out by means of SOURCEEXTRACTOR (Bertin & Arnouts, 1996) in dual mode, with the r filter acting as a reference image. Considering the distance of the galaxy and the mean effective radii of extragalactic GCs (e.g. Peng et al., 2008), they are not expected to be resolved for the typical seeing in these images and can be assumed as point-sources. For each filter we apply an aperture diameter close to three times the seeing of the image. Then, a selection of point-sources is done, based on the SOURCEEXTRACTOR parameters, FWHM and stellarity index, obtained from the r filter.

2.2. Photometric corrections

Several bright and isolated stars are used to calculate the aperture corrections in different sections of the fields. Then, zero points are calculated from the cross-match of the point-sources with the J-PLUS photometric catalogue. Finally, foreground extinction corrections are calculated for each source, taking into account a E_{B-V} map built from the extinction calculators of the NASA/IPAC Infrared Science Archive**, based on the Schlafly & Finkbeiner (2011) calibration, and the extinction coefficients for the J-PLUS filters from López-Sanjuan et al. (2019). We are aware sources embedded in the disk of both spirals are still affected by their intrinsic extinction.

3. Results

3.1. Selection of GC candidates

The point-sources catalogue is matched with Gaia EDR3 (Gaia Collaboration et al., 2021) to add information

**<https://irsa.ipac.caltech.edu/applications/DUST/>

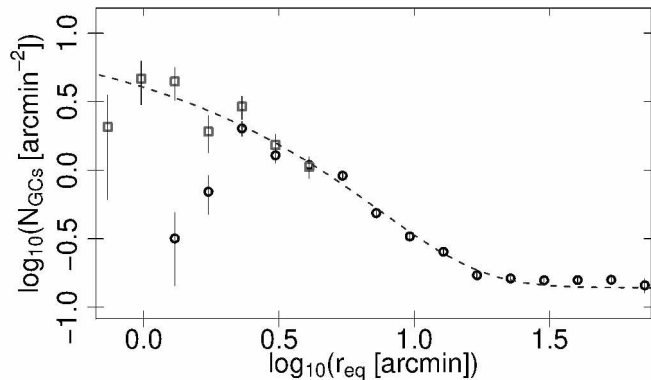


Figure 2: Radial profile for GC candidates, centred on M 81 (black circles). The green squares correspond to GC candidates in the inner region of M 81 (Nantais et al., 2011), where our completeness drops. The dashed blue curve represents a Sérsic law fitted to the profile.

on proper motions. Following Paper I, objects with $\mu > 3.6 \text{ mas yr}^{-1}$ are rejected. The GC candidates are selected from their colours (see Fig. 1), following typical ranges for old GCs (e.g. Ennis et al., 2020). These are also in agreement with colours of M 81 GCs from the literature (indicated in the figure with green squares). In addition, we restricted the sample to sources in the range of magnitudes $16 < i_0 < 20.75$. The bright limit restricts contamination from bright Galactic stars, at luminosity ranges where GCs are scarcely found (e.g. Harris et al., 2014). The faint limit is motivated by the completeness drop for lower luminosities.

3.2. Radial distribution

In Fig. 2 we show the radial distribution for GC candidates, centred on M 81. The GCs densities are obtained from elliptical rings, with ellipticity and position angle following those of M 81 disk. The black circles correspond to our photometry from the J-PLUS images. It is evident that the completeness decreases for galactocentric distances below 2.5 arcmin, where GCs are embedded in the disk of the galaxy. Hence, the analysis is complemented with GC candidates selected by colour and size criteria by Nantais et al. (2011) from HST/ACS images (green squares). A Sérsic law (Sérsic, 1968) is fitted to the profile, together with an additive constant, to account for the contamination level. The profile seems to flatten at galactocentric distances larger than ≈ 20 arcmin (i.e. $\approx 20 \text{ kpc}$ at M 81 distance). The numerical integration of the Sérsic law up to this limit results in ≈ 280 GCs brighter than $i_0 = 20.75$ mag. According to the GC luminosity function (GCLF) from Nantais et al. (2011), and assuming no significant variations of the GCLF for the outskirts, this represents ≈ 0.75 of the GCs, resulting in a population of ≈ 370 GCs. From the infrared magnitudes of M 81 indicated in the website of the NASA/IPAC Extragalactic Database***, and the relations from Bell et al. (2003), the galaxy has a stellar mass of $M_* \approx 6 \times 10^{10} M_\odot$. We adopt the pa-

***<https://ned.ipac.caltech.edu/classic/>

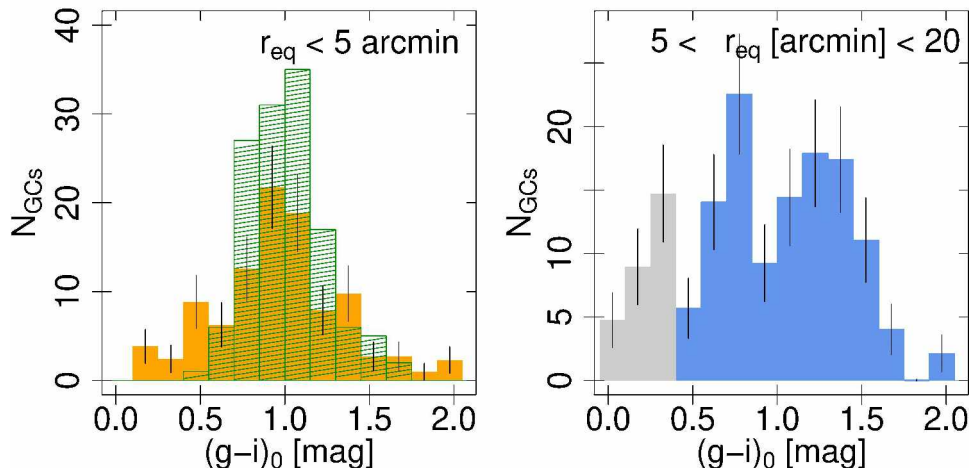


Figure 3: Colour distribution for GC candidates around M81, split into two radial regimes. In the *left panel*, the dashed histogram corresponds to GC candidates from Nantais et al. (2011) and the solid orange one to our J-PLUS photometry. In the *right panel*, the grey colour highlights the contribution with $(g-i)_0 < 0.5$ mag, that is due to presumably young stellar clusters, concentrated towards the spiral arms of M81.

parameter defined by Zepf & Ashman (1993) to measure the richness of GCS, leading to $T_N \approx 6$, which is an intermediate value for spiral galaxies in this mass range.

3.3. Colour distribution

The Fig. 3 shows the colour distribution of the GCs around M81, split into two radial regimes. The left panel corresponds to the region in common with Nantais et al. (2011). The orange solid histogram is built from our catalogue, and the green dashed one represents the GC candidates brighter than $i = 20.75$ mag from Nantais et al. (2011), with magnitudes converted from (V, I) to (g, i) by means of the equations from Bassino & Caso (2017). Although there are differences in completeness between the photometries from J-PLUS and HST/ACS, both samples are dominated by GCS with intermediate colours, and a bimodal distribution is not evident. The right panel corresponds to the colour distribution at larger galactocentric distances, up to the total extension of the GCS indicated in the previous section. It resembles a bimodal distribution, with peaks at $(g-i)_0 = 0.75$ mag and $(g-i)_0 = 1.2$ mag, respectively. These values are in agreement with typical mean colour for blue and red subpopulations of old GCs in the literature. The objects with $(g-i)_0 < 0.5$ mag are mainly concentrated towards the spiral arms of the galaxy, and are assumed to be young stellar clusters.

4. Summary

In this work we presented preliminary results of the analysis of the globular cluster system associated to

the spiral galaxy M81. The system has an extension of ≈ 20 kpc, a population of ≈ 370 GCs, and a colour distribution that behaves as unimodal in the portion embedded in the disk of the galaxy, and as bimodal in the outskirts.

References

- Bassino L.P., Caso J.P., 2017, MNRAS, 466, 4259
 Bell E.F., et al., 2003, ApJS, 149, 289
 Bertin E., Arnouts S., 1996, A&AS, 117, 393
 Cenarro A.J., et al., 2019, A&A, 622, A176
 Chies-Santos A.L., et al., 2022, MNRAS, 516, 1320
 de Blok W.J.G., et al., 2018, ApJ, 865, 26
 Ennis A.I., et al., 2020, MNRAS, 499, 2554
 Fensch J., et al., 2020, A&A, 644, A164
 Gaia Collaboration, et al., 2021, A&A, 649, A1
 Harris W.E., et al., 2014, ApJ, 797, 128
 Haslbauer M., et al., 2022, ApJ, 925, 183
 Kruijssen J.M.D., et al., 2019, MNRAS, 486, 3180
 Lomelí-Núñez L., et al., 2022, MNRAS, 509, 180
 López-Sanjuan C., et al., 2019, A&A, 631, A119
 Ma J., et al., 2017, MNRAS, 468, 4513
 Nantais J.B., et al., 2010, AJ, 139, 1413
 Nantais J.B., et al., 2011, AJ, 142, 183
 Oehm W., Thies I., Kroupa P., 2017, MNRAS, 467, 273
 Peng E.W., et al., 2008, ApJ, 681, 197
 Perelmuter J.M., Brodie J.P., Huchra J.P., 1995, AJ, 110, 620
 Schlafly E.F., Finkbeiner D.P., 2011, ApJ, 737, 103
 Sersic J.L., 1968, *Atlas de Galaxias Australes*
 Smrcina A., et al., 2020, ApJ, 905, 60
 Tully R.B., et al., 2013, AJ, 146, 86
 Villaume A., et al., 2020, ApJ, 900, 95
 Zepf S.E., Ashman K.M., 1993, MNRAS, 264, 611